Paper No. 25

A METHOD FOR PREDICTING BLAST WAVE OVERPRESSURE PRODUCED BY RUPTURE OF A GAS STORAGE VESSEL

P. W. Garrison, *McDonnell Douglas Astronautics Company*

ABSTRACT

A method, based on a hydrodynamic solution to the spherical shock problem, is developed to predict blast wave overpressure. Generalized curves are presented that permit the application of this technique to a wide range of pressure vessel sizes and pressures. Safety analyses of high pressure system failures are normally based on scaled explosive data (TNT scaling). An evaluation of available experimental data indicates that the hydrodynamic model provides a better approximation of blast overpressures generated when a pressure vessel ruptures.

NOMENCLATURE

A	ACOUSTIC VELOCITY	ft/sec
E	ENERGY	$ft\text{-}lb_f$
K	SPECIFIC HEAT RATIO	
M	MACH NUMBER	
P	PRESSURE	psfa
ΔP	STATIC OVERPRESSURE	psi
R	RANGE	ft
Ro	SPHERE RADIUS	ft
t	TIME	sec
V	VOLUME	ft^3

SUBSCRIPTS

i	INITIAL CONDITIONS
f	FINAL CONDITIONS
1	PRESHOCK CONDITIONS
4	INITIAL "DRIVER" CONDITIONS; i.e., INITIAL VESSEL CONDITIONS

INTRODUCTION

Gas storage vessels constitute a potential safety hazard to facilities and personnel. In order to establish safety requirements for the operation of these systems, it is necessary to predict the damage that might be sustained in the event of a system failure. In such an analysis, unjustified conservatism can result in costly constraints on test operations while the failure to recognize the full damage potential of a system can result in unnecessary risk.

Two basic damage mechanisms exist in any explosion. There is damage produced by the resultant shock wave and shrapnel damage caused by fragments of the pressure vessel. The scope of this paper will be limited to the shock wave and specifically to overpressure of the primary shock

522-137 O - 73 - 22

wave. A complete damage analysis requires consideration of blast wave impulse and positive phase duration as well as the natural and harmonic frequencies of the structure. Normally, this depth of analysis is not justified and incident overpressure in conjunction with established damage threshold data, Table I, is sufficient to establish safety criteria.

TABLE I
BLAST DAMAGE DATA

Type of Damage	Side-On Overpressure	Reference
Window Breakage (Lower Limit)	0.2	11
Structural Damage (Lower Limit)	0.4	11
Plaster Cracking	0.54	11
Eardrum Rupture	2.5	9
Lung Damage	6.0	9

TNT SCALING

The characteristics of the blast wave produced by the sudden release of a high pressure gas can be approximated by considering the blast produced by an "equivalent" amount of TNT. Expansion of a high pressure gas represents the release of energy. The magnitude of this energy is not only a function of initial and final pressures but is also a function of the thermodynamic path of the process. For a quasi-static expansion,

$$E = \int_{V_i}^{V_f} p\,dv \tag{1}$$

If an isentropic expansion of a calorically perfect gas is assumed, the available energy may be expressed:

$$E = \frac{V_i P_i}{K-1}\left[1 - \frac{P_i}{P_f}^{\frac{1-K}{K}}\right] \tag{2}$$

In Figure 1 is presented the energy density (E/V) associated with the expansion of a gas from some initial pressure to a final pressure of one atmosphere. This energy can be expressed in terms of an equivalent weight of TNT(W_{TNT}). For this purpose, 1.0 lbm of TNT (Symmetrical Trinitrotoluene) is assumed to generate 1.425×10^6 ft-lb of energy.

Experimental TNT overpressure data are presented in Figure 2 for free air and surface bursts. The higher overpressures exhibited by the latter are the result of interactions between the incident shock wave and the ground. The effect of such interactions is to increase the apparent yield of the explosion. A completely unyielding surface, one that absorbs no energy from the explosion, effectively doubles the apparent yield by concentrating the released energy into a single hemisphere. Typical apparent yield factors range from 1.5 to 2.0 (Ref. 7).

The characteristics of a blast wave are unchanged if the scales of length and time by which they are measured are changed by the same factor as the dimension of the explosive charge. Therefore, two explosions which differ only in energy release will exhibit identical blast wave intensities at

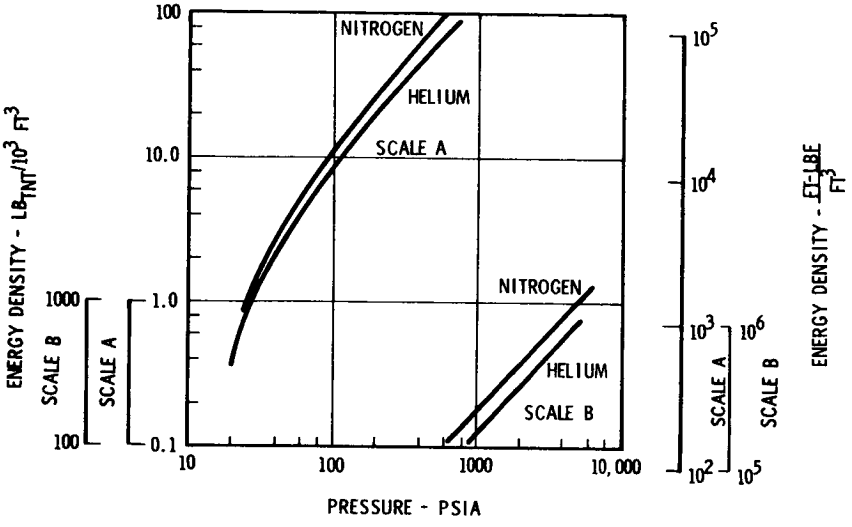

Figure 1. Pressure Vessel Energy

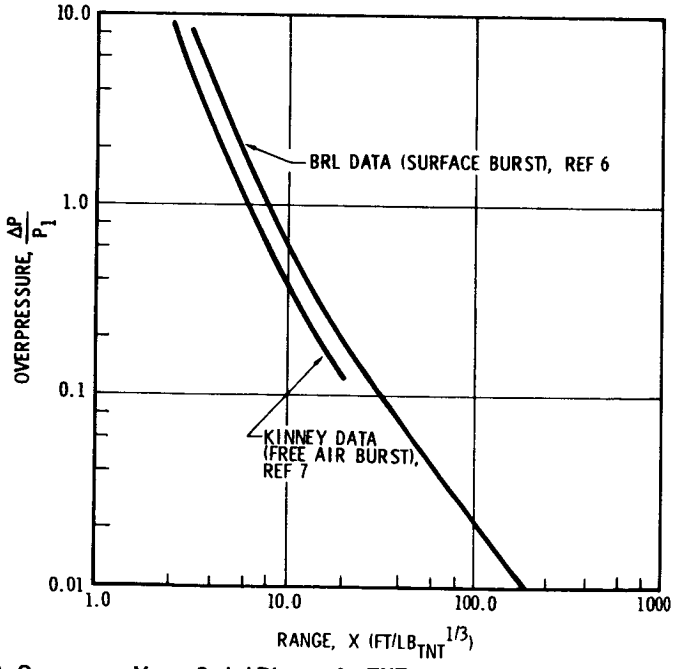

Figure 2. Overpressure Versus Scaled Distance for TNT

distances which are proportional to the cube root of the respective energy yields. This is expressed in terms of a range parameter, X, defined:

$$X = R/(W_{TNT})^{1/3} \tag{3}$$

TNT scaling permits the application of the data in Figure 2 to a wide range of explosive yeilds.

There is some question about the "equivalency" of a high explosive blast and the blast produced by the rupture of a pressure vessel. In a high explosive blast, a region of high pressure, high temperature gas is rapidly generated and subsequently expands into the surrounding environment. It is unlikely that the thermodynamic path followed by this process is the same as that followed by the "cold" gas of the latter case.

CHARACTERISTICS OF THE SPHERICAL SHOCK WAVE

The rapid release of a gas at an initial pressure in excess of atmospheric pressure is characterized by the formation of a spherical shock wave which propagates into the surrounding medium. As in the one dimensional problem, a centered expansion wave simultaneously propagates into the high pressure region. Unlike the one dimensional problem, a left facing secondary shock wave originates from the tail of the expansion wave, reflects from the orgin as a right facing shock wave, and subsequently trails behind the primary shock wave, (Figure 3). The study will be confined to the primary shock wave which is of major concern in damage analysis.

There is an important difference between the one dimensional problem as characterized by the shock tube and the spherical shock problem. The former exhibits a constant shock intensity and the latter a rapid decay of shock intensity with distance. This decay is the result of the three-dimensionality of the spherical flow. The evolution of a spherical shock wave is illustrated in Figure 4. Here, a quantity of gas at a pressure in excess of atmospheric pressure is allowed to

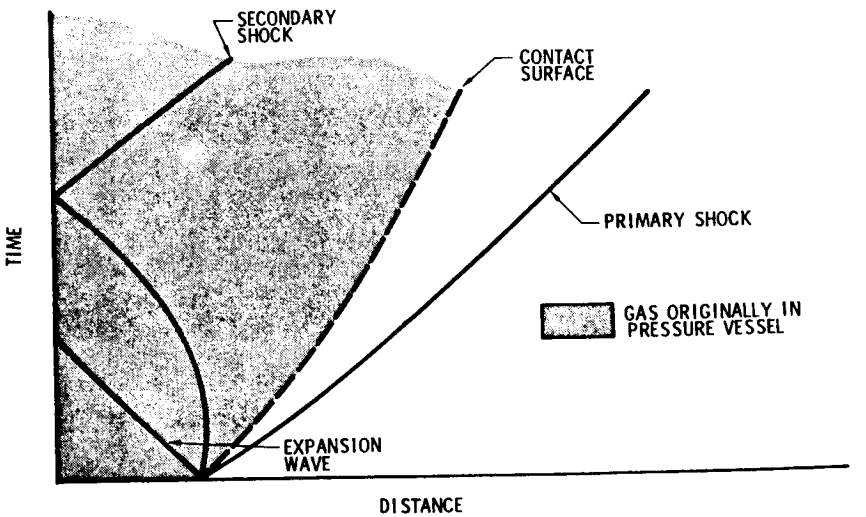

Figure 3. Space-Time Plot for Spherical Shock Wave

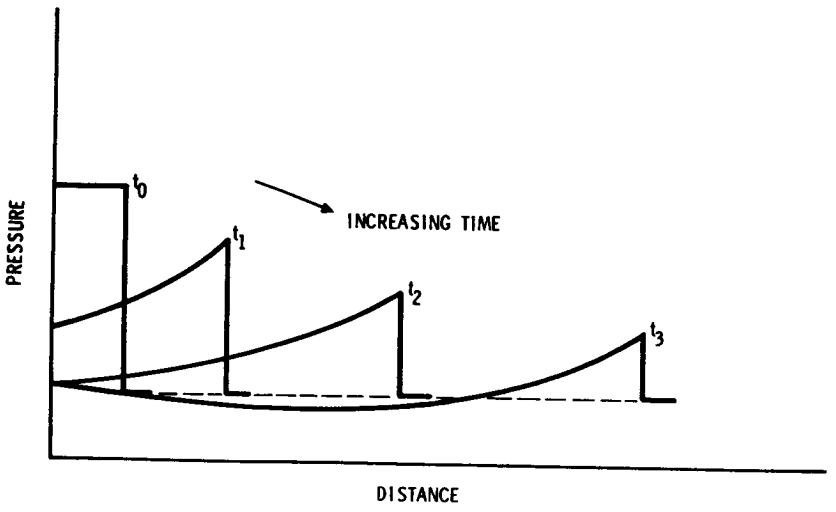

Figure 4. Overpressure Versus Distance

expand into the surrounding environment. The pressure disturbance is characterized by positive pressure discontinuity followed by a negative pressure phase of considerably less magnitude. The pressure history at a fixed station is depicted in Figure 5.

Along a streamline, a sphereical shock is locally indistinguishable from a one dimensional normal shock such that jump conditions can be computed from the Rankine-Hugoniot relation.

$$\frac{\Delta P}{P_1} = \frac{2K_1(M^2-1)}{K_1+1} \tag{4}$$

Equation (4) gives the increase in static pressure across the shock front (overpressure) as a function of shock mach number.

HYDRODYNAMIC MODEL

A mathematical description of the spherical blast wave requires the solution of the full set of nonlinear partial differential equations representing conservation of mass, momentum and energy. Similarity solutions were first obtained for the hypothetical point source explosion by Von Neumann and Taylor. Brode (Ref. 3 and 4) developed a numerical solution to the finite source explosion based on the numerical integration of a set of finite difference equations for a specific set of initial and boundary conditions. Witham later developed an approximate set of differential equations which describe the relationship between shock strength and area for a shock wave moving through a channel with a varying cross-sectional area. Friedman's (Ref. 5)

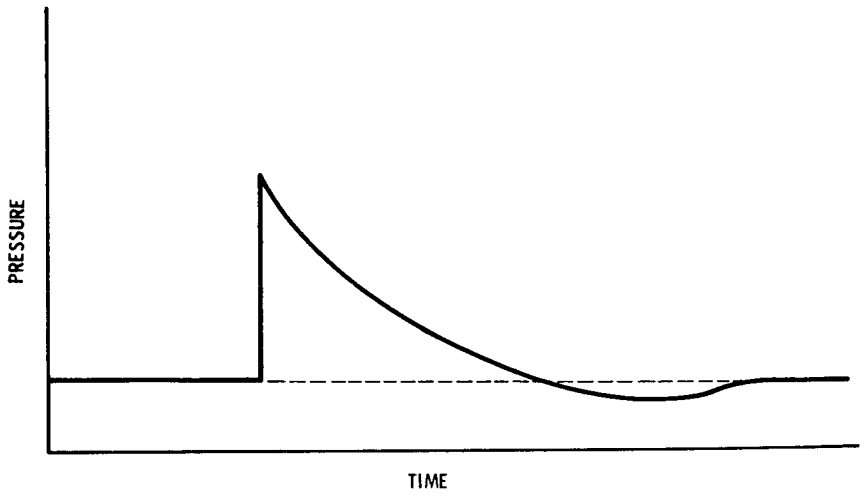

Figure 5. Overpressure at a Fixed Station

successful integration of these equations lead to the following closed form solution for the finite source problem:

$$\left(\frac{R^2}{R_0}\right)\frac{(Y-Z)^2}{M}\left[(K-1)^{1/2}Y+(2K)^{1/2}Z\right]^{(2K/(K-1))^{1/2}}Y^{2/K} \cdot \text{EXP}\,(2K-2)^{-1/2}\,\text{SIN}^{-1}\left[\frac{2Y^2-(K-1)Z^2}{(K+1)^2M^2}\right] = \text{CONSTANT} \tag{5}$$

$$Y^2 = 2KM^2 - K+1$$

$$Z^2 = (K-1)M^2+2$$

Given the initial position and magnitude of the shock wave, equation (5) can be used to describe the subsequent shock history. These initial conditions can be obtained from the one-dimensional shock tube equation.

$$\frac{P_4}{P_1}\left[1-\frac{A_1}{A_4}\frac{K_4-1}{K_1+1}\left(M-\frac{1}{M}\right)\right]^{2K_4/(K_4-1)} = \frac{2K_1M^2-K_1+1}{K_1+1} \tag{6}$$

Equation (6) is presented graphically in Figure 6 for nitrogen and helium drivers (Region 4). In this equation, Region (4) refers to conditions in the unruptured pressure vessel and Region (1) refers to the external environment into which the shock propagates. From this equation, the

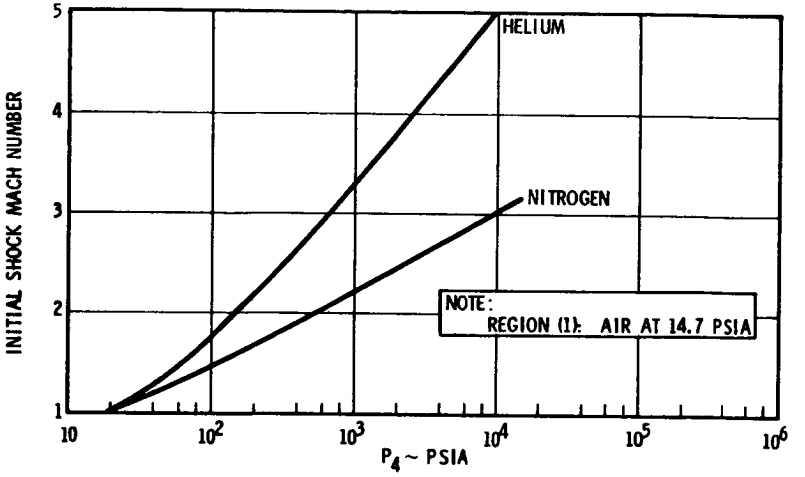

Figure 6. Initial Shock Intensity Versus Burst Pressure

initial mach number at $R/R_0 = 1$ can be computed and the constant of integration in equation (5) can be evaluated. Once the mach number at a given station is established, equation (4) can be employed to compute the corresponding overpressure. Solutions to equations (4) through (6) are presented in Figures 7 and 8 for helium and nitrogen drivers (Region 4). In both cases, the Region (1) medium is assumed to be air at one atmosphere.

It should be emphasized that the Friedman-Witham solution is approximate and does not take into account the weakening effects of disturbances which originate in the flow field behind the shock wave. Brode's numerical solution does account for these effects and differs only slightly from the approximate theory in its description of the initial motion of the shock wave. The effects of such disturbances can become more pronounced at distances far removed from the blast. Care should be exercised, therefore, in applying the model at ranges significantly beyond those verified by data.

EXPERIMENTAL DATA

Experimental data from four sources are summarized in Table II. Boyer's data (Ref. 1 and 2) are based on small glass spheres which were pressurized (326 psia and 400 psia) with air and ruptured in a one atmosphere (air) environment. Kornegay's experiments (Ref. 8) also utilize small glass spheres. These spheres were filled with air at approximately one atmosphere and ruptured in a low pressure chamber at 2.0 and 5.0 torr. The Pittman data (Ref. 10) are based on the burst tests of five full scale pressure vessels. Burst pressures ranged from 640 to 8145 psia. The Altas data (Ref. 9) are included to demonstrate the application of the two blast models to a large scale pressure vessel. These data were obtained from the explosive failure of a full scale missile pressurized to 49.7 psia with nitrogen.

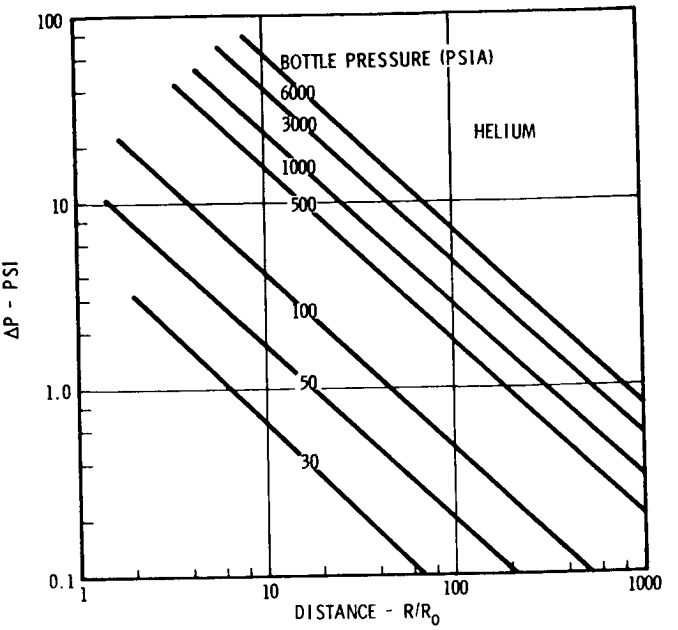

Figure 7. Blast Wave Overpressure for Bottle Rupture — Friedman Witham Model

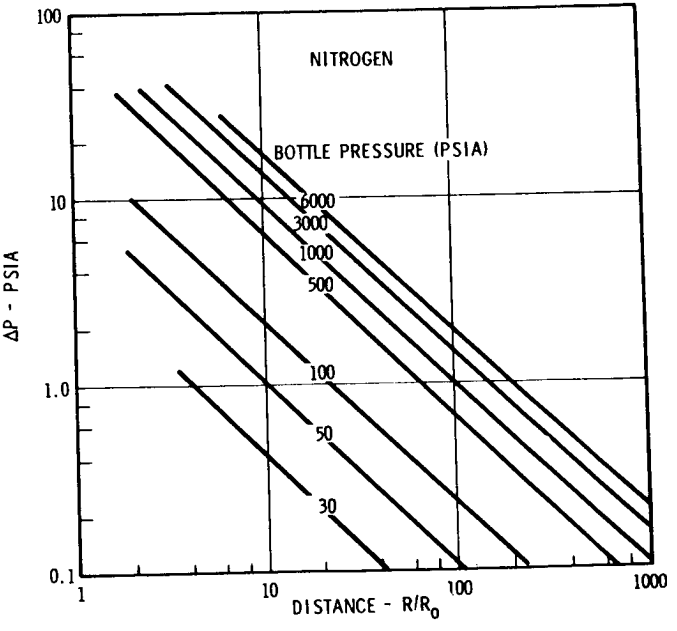

Figure 8. Blast Wave Overpressure for Bottle Rupture — Friedman-Witham Model

TABLE II
EXPERIMENTAL DATA

Source	Run	Volume (ft^3)	R_o (ft)	Gas	P_4/P_1	P_4 (psia)	E (lbs TNT)
Atlas (Ref. 9)		4050.0	9.89	N_2	3.38	49.7	14.9
Boyer (Ref. 1 & 2)	a	2.27×10^{-3}	0.0815	Air	22.2	326	1.1×10^{-4}
	b	2.27×10^{-3}	0.0815	Air	27.2	400	1.4×10^{-4}
Kornegay (Ref. 8)	a	1.37×10^{-4}	0.032	Air	425	16.4	1.78×10^{-4}
	b	1.37×10^{-4}	0.032	Air	130	12.6	4.97×10^{-5}
Pittman (Ref. 10)	a	1.34	0.684	N_2	43.5	640	0.143
	b	1.68	0.738	N_2	41.8	615	0.171
	c	0.235	0.383	N_2	545	8015	0.397
	d	6.0	1.127	N_2	545	8015	10.14
	e	6.0	1.127	N_2	554	8145	10.3

Calculations based on TNT scaling and the hydrodynamic model have been made for inital conditions corresponding to the experimental data. In each case, lower overpressures are predicted with the hydrodynamic model than with TNT scaling for the initial stages of the blast wave. For the TNT model, decay is more rapid as the shock propagates outward. At distances removed from the origin, overpressures are predicted with the hydrodynamic model that exceed those indicated by TNT scaling.

In applying the hydrodynamic solution to non-spherical pressure vessels, it has been assumed that the blast wave assumes the characteristics of wave produced by a spherical vessel of the same volume at some distance from ground zero.

No attempt has been made to account for the kinetic energy associated with the fragments of the pressure vessel produced by the explosion. This represents a reduction in the energy associated with the blast wave but is a quantity that cannot easily be established. Based on Schlieren records (Ref. 1), Boyer estimates that 16 percent of the total energy is found in the kinetic energy of the fragments. It appears likely that the percent of the total energy that is transferred to the fragments is not constant but is a function of the failure mechanism, tank geometry, and tank material. In this report, the conservative approach will be taken, i.e., it will be assumed that all the energy is involved in the blast wave. The uncertainty associated with this variable may be responsible for some of the scatter observed in the experimental data presented.

Blast wave interaction with the ground plane must be taken into account for the Pittman and Atlas data (Ref. 9 and 10). For these cases, the BRL surface burst data (Figure 2, Ref. 6) is used

for TNT scaling. The hydrodynamic model does not account for interactions between the blast wave and the ground plane. Therefore, an apparent yeild factor must be established to account for this effect. During the Pittman test, a series of known TNT charges were exploded to evaluate the interaction coefficient. From these data, a coefficient of 1.5 was determined. This apparent yeild factor was used in conjunction with the hydrodynamic model for both the Pittman and Atlas calculations. The effective pressure vessel volume for these tests is 1.5 times the actual volume. The range scale computed by the hydrodynamic model (free air burst) is increased by a factor of $(1.5)^{1/3}$ to account for the ground effect.

Figures 9 through 15 present data from these four sources and corresponding predictions based on TNT scaling and the hydrodynamic model. The Atlas data (Figure 9) falls in a region where the two models are indistinguishable and provide no information concerning the relative merit of the two models. It does, however, demonstrate that overpressure prediction techniques under investigation can provide a reasonable approximation of blast wave overpressure for a large volume (4050 ft^3), low pressure (49.7 psia) tank rupture.

Boyer's data (Figures 10 and 11) were taken in the region where the hydrodynamic solution exceeds the TNT model. These data fall below the TNT prediction. Insufficient data were taken to provide any information concerning the relationship between overpressure and range.

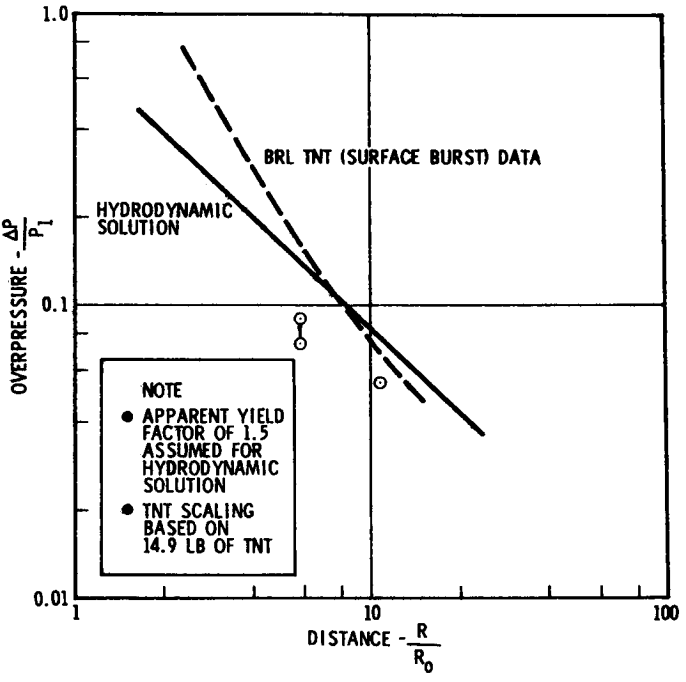

Figure 9. Atlas Data

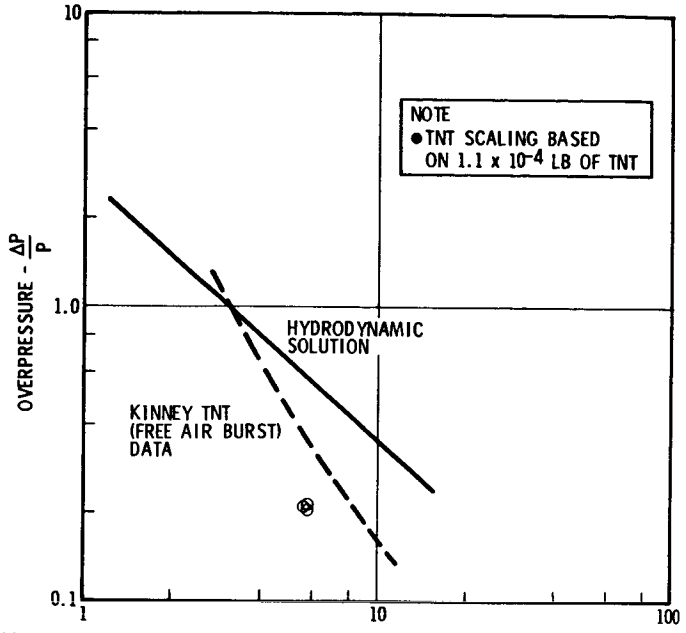

Figure 10. Boyer Data — Run (A)

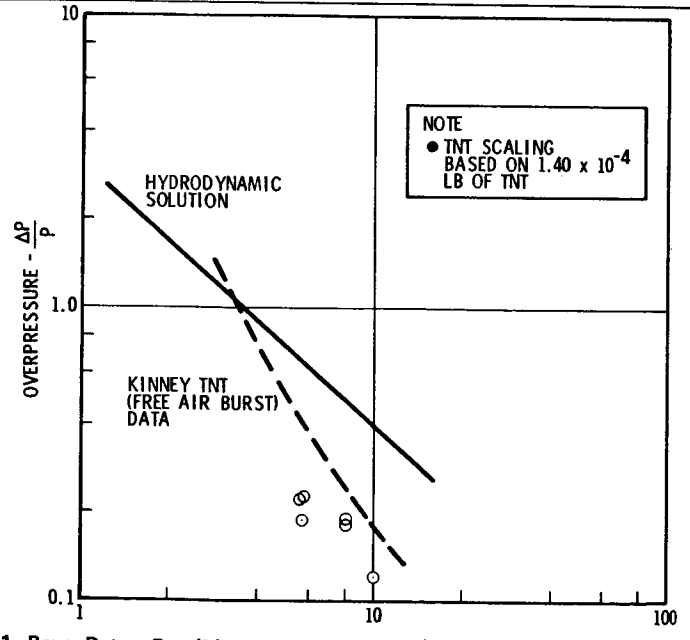

Figure 11. Boyer Data — Run (B)

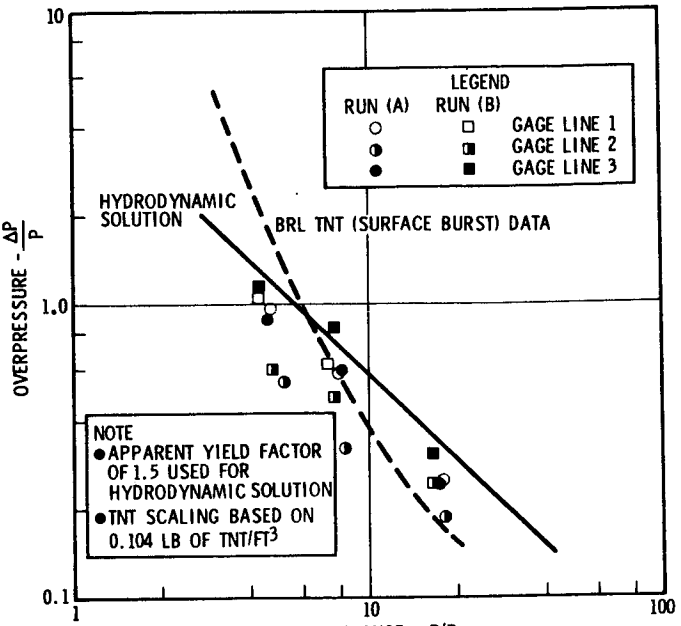

Figure 12. Pittman Data – Run (A) and (B)

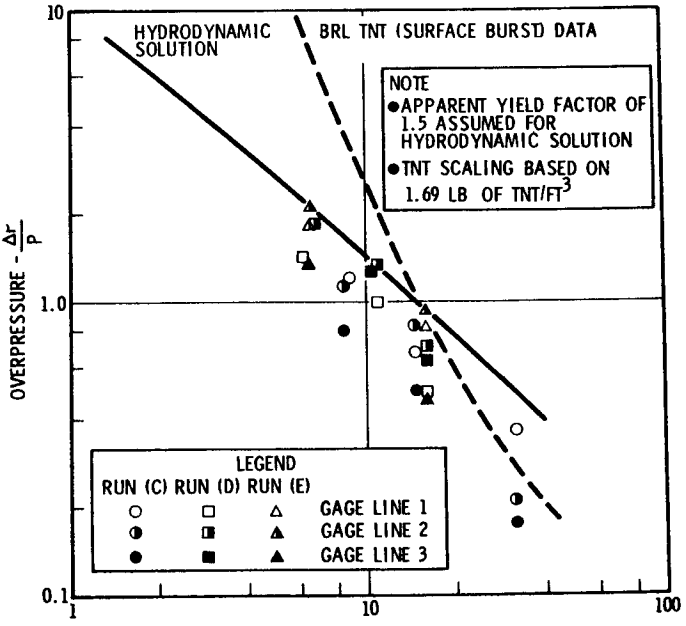

Figure 13. Pittman Data – Runs (C) – (E)

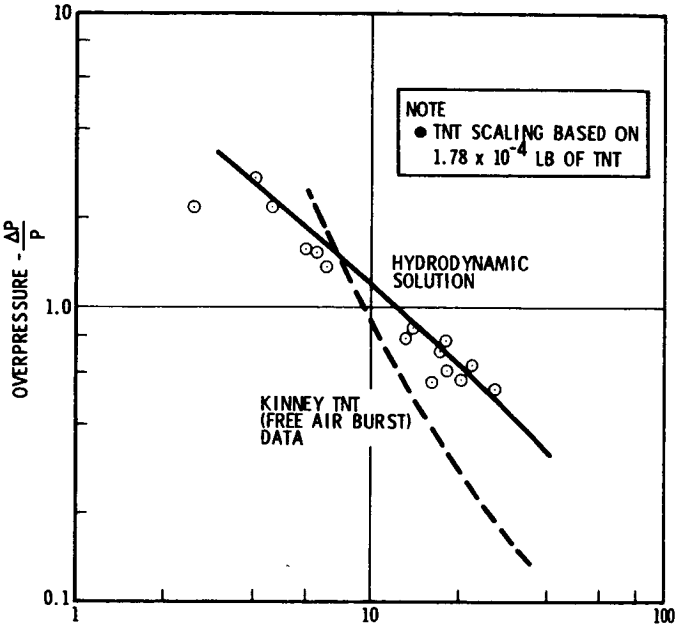

Figure 14. Kornegay Data – Run (A)

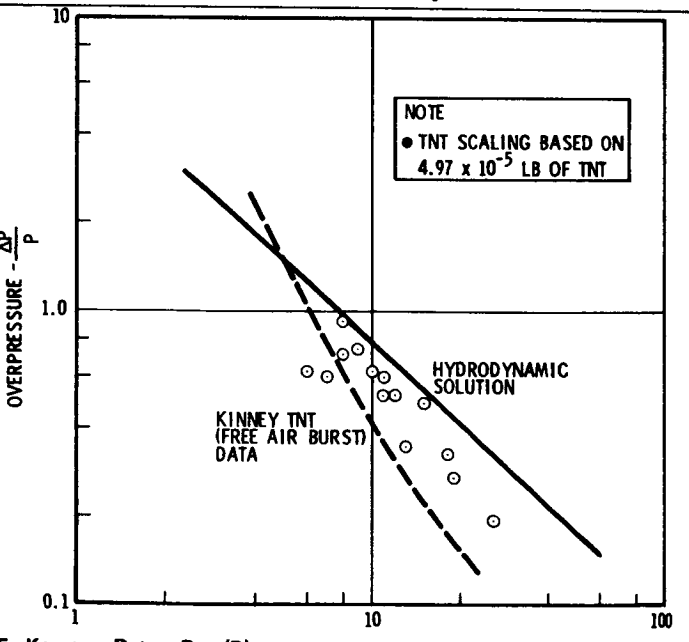

Figure 15. Kornegay Data – Run (B)

Two of Pittman's tests (Figure 12) were conducted at burst pressures (640 psia and 615 psia) not significantly different from those of the Boyer test (326 psia and 400 psia). Pittman's data, taken in this same region (R/R_0), fall above the level predicted by TNT scaling. Pittman's data taken near the orgin are significantly less than that predicted by TNT scaling and agrees well with the hydrodynamic model. Pittmann's three tests conducted at approximately 8000 psia (Figure 13) follow the same trend and provide a large number of data points which support the lower overpressure predicted by the hydrodynamic model for stations near the origin. Pittman's data were taken along three equally spaced radial lines extending from the center of the pressure vessel. Different overpressures were measured along different gage lines. A lack of symmetry in the shock front is indicated. This asymmetry is most likely a result of the asymmetric failure of the pressure vessel.

Kornegay's experiments, Figure 14 and 15 were conducted at moderate pressure ratios (P_4/P_1 = 130 and 425). These data agree quite well with the magnitude and slope predicted by the hydrodynamic model.

CONCLUSION

This analysis indicates that the TNT scaling technique does not adequately describe the pressure vessel burst problem. Overpressures predicted by this method are unrealistically high for stations near the pressure vessel and too low for stations far removed. The hydrodynamic solution (Friedman-Witham) provides a better correlation with available data in both regions.

Overpressure is directly related to damage potential in an accidental rupture of a pressure vessel. If the region of interest is near the blast, the proposed method, Figures 7 and 8, may permit some relaxation of constraints placed on test operations by conventional blast analysis (TNT scaling). At distances removed from the blast, the hydrodynamic model will assure that the full potential of the blast wave is taken into account. The hydrodynamic solution (Friedman-Witham) presented in this report is approximate and may be overly conservative at distance significantly beyond those empirically verified.

REFERENCES

1. D. W. Boyer, H. L. Brode, I. I. Glass, and J. G. Hall. Blast from a Pressurized Sphere. University of Toronto Institute of Aerophysics, Report No. 48, January 1958.

2. D. W. Boyer. An Experimental Study of the Explosion Generated by a Pressurized Sphere. Journal of Fluid Mechanics, August 16, 1960.

3. H. L. Brode. Numerical Solution of a Spherical Blast Wave. Report No. P-452, The Rand Corporation, Santa Monica, California, November 10, 1953.

4. H. L. Brode. The Blast from a Sphere of High Pressure Gas. Report No. P-582, The Rand Corporation, Santa Monica, California, January 27, 1955.

5. M. P. Friedman. A Simplified Analysis of Sperical and Cylindrical Blast Waves. Journal of Fluid Mechanics, Volume II, 1961.

6. C. N. Kingery and B. F. Pannill. Peak Overpressure vs. Scaled Distance for TNT Surface Bursts (Hemispherical Charges). BRL Memorandum Report No. 1518, Ballistic Research Laboratories, Aberdeen Proving Grounds, Maryland, April 1964.

7. G. F. Kinney. Explosive Shocks in Air. The MacMillan Company, New York, 1963.

8. W. M. Kornegay. Production and Propagation of Spherical Shock Waves at Low Ambient Pressures. Technical Report 375, Massachusetts Institute of Technology, Lincoln Laboratory, Lexington, Massachusetts, January 26, 1965.

9. H. Moskowitz. Blast Effects Resulting from Fragmentation of an Atlas Missile. AIAA Paper No. 65-195, AIAA/NASA Flight Testing Conference, Huntsville, Alabama, February 15-17, 1965.

10. J. F. Pittman. Blast and Fragment Hazards from Bursting High Pressure Tank. Report No. NOL-TR-72-102, May 17, 1972.

11. Criterion For Locating SIVB Testing Facilities at SACTO, Douglas SM42365, September 1962.